J. Phys. Chem. Solids, 1973, Vol. 34, pp. 687–703. Pergamon Press. Printed in Great Britain

HYDROSTATIC PRESSURE DERIVATIVES OF THE SINGLE CRYSTAL ELASTIC MODULI OF Gd, Dy AND Er*

E. S. FISHER†, M. H. MANGHNANI and R. KIKUTA
University of Hawaii, Hawaii Institute of Geophysics, Honolulu, Hawaii 96822, U.S.A.

(*Received* 27 *March* 1972)

Abstract—The hydrostatic pressure derivatives of the single crystal elastic moduli of Gd, Dy and Er have been measured at 298°K, to pressures near 5 Kbar. The very small pressure derivatives of the adiabatic bulk moduli indicate that a small ion core model should be appropriate for interpreting the data. The long-range electrostatic contributions to the shear moduli have a dominant influence on the pressure derivatives of the shear moduli of Er, whereas the Gd and Dy data evidently reflect band structure contributions. The values of the longitudinal stiffnesses correspond remarkably well with the Bohm–Staver model for velocity of waves in an ion plasma dispersed in a sea of electrons, where the ionic interaction is purely Coulombic. This model is extended to provide an interpretation of the volume derivatives of the longitudinal moduli in terms of the volume derivative of the density of electron states at the Fermi energy.

The Grüneisen parameters calculated from averages of the acoustic model gammas are in relatively poor agreement with those determined from thermal expansion data. An explanation based on the changes in c/a ratio with volume change is tested quantitatively and found to be reasonably successful. The values of dK_T/dP, where K_T is the isothermal bulk modulus, are applied to the Murnaghan equation of state and give excellent agreement with Bridgman's direct compression data for Dy and Er to 40 Kbar. For Gd, Bridgman's data indicate either that $(dK_T/dP)_{P=0}$ should be considerably larger than deduced from the adiabatic dK_s/dP measurements or that a phase change occurs near 20 Kbar. The occurrence of a phase change in Er at ~ 90 Kbar is definitely indicated when comparing the Murnaghan equation with X-ray diffraction data.

1. INTRODUCTION

MEASUREMENTS of the hydrostatic pressure derivatives of elastic moduli in ionic crystals have proven to be invaluable in testing the validity of the simple central force Born model, where one is concerned with an electrostatic potential that is $1/r$ dependent and a repulsive potential varying as $1/r^n$. The values of the exponent n deduced from such work have provided a basis for understanding several properties of ionic materials that are of broad interest [1]: (a) the variations of dK/dP and $d\mu/dP$, where K is the bulk modulus and μ is the isotropic shear modulus, with composition and crystal structure, (b) the anisotropy in the single crystal shear moduli and their pressure derivatives, and (c) the variation in the Grüneisen parameter, γ. In metals the extraction of information from the elastic moduli and their pressure derivatives is, in general, considerably more complex because of the free electron and band structure contributions, that presumably become more important in the higher order elastic moduli [2]. There are, nevertheless, some extreme cases such as the noble metals where the core repulsion has a dominating influence and the third-order elastic moduli or the dc_{ij}/dP can be useful in evaluating the repulsive potentials [3]. In the opposite situation where the ion cores are widely separated, the shear moduli are almost totally given by the electrostatic component,

$$c_{ij}^e = \frac{M_{ij} Z_{\text{eff}}^2}{\Omega_0 r_0}, \quad i = j \tag{1}$$

*Hawaii Institute of Geophysics Contribution No. 420.

†Visiting Professor, Permanent Address: Materials Science Division, Argonne National Laboratory, Argonne, Ill. 60439, U.S.A.

where, M_{ij} is a Coulomb sum factor that depends on structure and mode of shear strain, Z_{eff} is the effective valence on the ion, Ω_0 is the atomic volume and r_0 is the undeformed ionic radius. The volume derivatives of the shear moduli in such cases should correspond to

$$\pi_{ij}^e = \frac{\mathrm{d} \ln c_{ij}^e}{\mathrm{d} \ln V} = -\frac{4}{3} \tag{2}$$

where V is the total volume and M_{ij}^e and Z_{eff} are assumed independent of V. In several metals where equation (2) may be expected to hold, the experimental data indicated that factors other than the electrostatic forces dominate the $\mathrm{d}c_{ij}/\mathrm{d}P$. In the bcc alkali metals [2], for example, the values of c_{44} and c' are almost completely derived from equation (1), whereas the values for π_{44} and $\pi_{c'}$ in Na and K are about a factor of two greater in magnitude than the $-4/3$ given by equation (2). These large deviations are attributed either to the effects of volume on the band structure contributions or to changes in Z_{eff} with volume. The deviations from the purely electrostatic model are even more pronounced in the polyvalent cases of A1 and Mg, where again the repulsive potential has only a minor role but the band structure effects on the pressure derivatives of the model are very large [4].

The rare earth metals form another group where the electrostatic potential can be expected to have a dominant influence on the elastic moduli at least in the paramagnetic structures. The principal magnetic properties of the heavy rare earths in particular, Gd through Tm, conform to a simple model of tripositive ions embedded in a sea of $5d$ and $6s$ valence electrons. Since the $4f$ electrons are closely bound to the ions with radii considerably smaller than the interatomic radii, the ionic repulsion should be a minimum factor in the bonding, as in the alkali metals. The values of the second order c_{ij} in these hexagonal close packed (*hcp*) structures, together with recent calculations by Cousins [5], do in fact indicate that the repulsive potentials play a minor role and that this simple electrostatic model is nearly sufficient to explain the variation of the shear moduli with atomic number. Cousins has computed Coulomb sum factors, M_{ij}, for the three principle shear moduli in *hcp* structures as a function of the axial, c/a, ratio. If we use these values of M_{44} in equation (1), together with a $Z_{\text{eff}} = 3$ we find, for example, that the electrostatic contributions to c_{44}, c_{44}^e, for Gd, Dy, Ho and Er are at most 30 per cent larger than the measured room temperature values [6–9]. The measurements of the hydrostatic pressure derivatives of the shear moduli in Gd, Dy, and Er that are reported here provide a more sensitive test of the electrostatic model and also provide some information in regard to the importance of the band structure energy in evaluating the effects of pressure on other properties of rare earth metals.

The value of M_{ij} to be used in equation (1) will necessarily change with c/a ratio in *hcp*, or any uniaxial, crystal. In such crystals the isothermal linear compressibilities parallel and perpendicular to the 'c' axes, $\beta_{\|}$ and $\beta_{\perp}$, respectively, generally are different in magnitude. This produces a change in c/a ratio with hydrostatic pressure and introduces a small change in equation (2) for uniaxial crystals, where

$$\pi_{ij}^e = \frac{\mathrm{d} \ln c_{ij}^e}{\mathrm{d} \ln V} = -\frac{4}{3} + \left(\frac{\partial M_{ij}}{\partial (c/a)}\right)_V \times \frac{c/a}{M_{ij}} (\beta_{\|} - \beta_{\perp})/\beta_V \tag{3}$$

and β_V is the isothermal volume compressibility. A recent analysis of the measured $\mathrm{d}c_{44}/\mathrm{d}P$ values for *hcp* Ti and Zr metals [10] suggested that the second term on the right of equation (3) has a very prominent effect in determining whether c_{44} increases or decreases with volume. This term also becomes somewhat significant in influencing $\mathrm{d}c_{44}/\mathrm{d}P$ in Gd

and Er and becomes very important in the interpretation of the differences between the Grüneisen parameter, $\bar{\gamma}_H$, as calculated from the averaging of the mode γ's that are based on the present experimental data and the $\gamma_H(\alpha_V)$ that are derived from thermal expansion and heat capacity measurements. The mode gammas are derived here from a modification of the following equation that applies to cubic symmetry [11]:

$$\gamma_i = -\frac{1}{6} + \frac{1}{2}\left(\frac{\partial \ln c_i}{\partial \ln V}\right)_T \qquad (4)$$

where i refers to a specific normal mode of vibration in a given crystallographic direction and c_i is the stiffness modulus for this mode.

In addition to the electrostatic contribution to the pressure derivatives of the shear moduli, c_{44}, c_{66} and $C_H = 1/6\ (c_{11}+c_{12}+2c_{33}-4c_{13})$, we have here attempted to calculate the screened electrostatic contributions to dc_{11}/dP and dc_{33}/dP, (pressure derivatives of the longitudinal modes) via the Bohm–Staver [12] formula for the vibrational frequency of metal ions in an electron plasma. This appears to be a novel but simple approach that may prove useful in extracting valuable information regarding the contribution of the electronic Grüneisen γ, γ_e, to the γ_i for longitudinal modes of lattice vibration.

2. EXPERIMENTAL PROCEDURES

The Gd, Dy and Er single crystals that were used in this study were precisely those used in earlier studies [6, 7] of the temperature dependence of the c_{ij}. The Dy crystals were prepared by prolonged annealing of an arc melted button obtained from pure sponge material. Because the ultrasonic wave velocities in Dy appeared to be uniquely sensitive to purity, as described in Ref. [7], a special effort was made to prepare relatively clean single crystals where the cross-checks on the various moduli were consistent to within 0·3 per cent. The Er and Gd crystals were made by a similar annealing procedure, but the starting materials were made by casting into Ta crucibles. The single crystals did contain a large number of microscopic inclusions, presumed to be complex compounds containing Ta, but the cross-checks on the zero pressure wave velocities indicated no significant effects of the impurities.

Three crystals of each metal were prepared for propagating waves parallel, perpendicular and near 45° of arc to the 'C' axis, i.e. hexagonal, axis. Table 1 relates the elastic moduli measured in the experiments to the crystal and transducer orientations. The ultrasonic path lengths varied from 2 to 3 mm, among the crystals used in this study.

The apparatus for measuring the wave velocities under hydrostatic gas pressures up to 72,000 psi, or 4·964 Kbar is described in a prior publication [13]. Briefly, this consisted of an ultrasonic pulse superposition machine with carrier r.f. frequencies of 30 MHz.

Table 1. Relations of measured wave velocities to elastic stiffness moduli

Crystal specimen	Direction of wave propagation	Type of mode	Direction of particle motion	Elastic modulus determined from measured velocity
A	⊥ to "C"	long.	⊥ to "C"	c_{11}
	⊥	shear	∥	c_{44}
	⊥	shear	⊥	c_{66}
B	~ 45°	long.	45°	c_{RS}*
C	∥	long.	∥	c_{33}
	∥	shear	⊥	c_{44}

*$c_{RS} = \frac{1}{4}(c_{11}+c_{33}+2c_{44}+[(c_{11}-c_{33})^2+4(c_{13}+c_{44})^2])^{1/2}$.

Temperatures were carefully regulated at $298 \pm 0{\cdot}1$°K.

The process of evaluating wave velocity and modulus changes from the changes of p.r.f. (pulse repetition rate frequency) with pressure is also described in Ref. [13]. This procedure is essentially based on recomputing the linear and volume compressibilities at steps of 4000 psi, 0·267 Kbar, so as to closely approximate the path length and density at each data point. The data points used for the calculations were, in turn, taken from linear equations obtained by a least-square fit to the initial data. The coefficients of correlation, r, or the estimated probable error for each data point, based on regression analyses for each set of data, provide the basis for the estimated probable errors in dc_{ij}/dP that are given in the results.

3. RESULTS

(a) *Zero pressure results*

The *hcp* rare earth metals display a variety of ordered magnetic arrangements [14]. The highest ordering temperature among this group occurs at Gd, (element 64) and decreases with increasing atomic number. Gadolinium goes directly from the paramagnetic state to a ferromagnetically ordered state, with T_c at approximately 291°K for the crystals used here [15]. There are indications, however, that some degree of spontaneous magnetic moment ordering exists at temperatures above T_c, extending to about 330°K [16]. This short range interaction between the ions, or between the conduction electrons and the ions, manifests itself, at $T > T_c$, in the lattice properties as an anomalous thermal expension at zero magnetic field with the c_0 lattice constant expanding with decreasing temperature. The modulus c_{33} is strongly influenced by the anomalous thermal expansion and dc_{33}/dT has a positive value at 298°K. The dc_{ij}/dT for the other principal moduli are, however, not significantly affected by the preliminary magnetic interactions and show significant changes only at T_c, as shown in Fig. 1. (These data were previously published in a conference proceedings [6] and are shown here because the values of dc_{ij}/dP at 298°K may well be influenced by the close proximity of T_c to the temperature of measurement). Hydrostatic pressures have the effect of decreasing T_c in Gd at the rate of $1{\cdot}5 \pm 1$°K per Kbar [17]. Some measurements of the effect of pressure on the variation of c_{33} at T near T_c are reported in Ref. [15].

The Curie temperature, T_c, of Dy is 87°K, but an antiferromagnetically ordered phase exists between the paramagnetic and ferromagnetic state. Between 87 and 179°K the magnetic moments are aligned parallel within each basal plane, but the difference in direction of alignment in adjacent basal planes produces a helix, or spiral, magnetic structure, with a temperature dependent turn angle. The large effects of these phase changes on

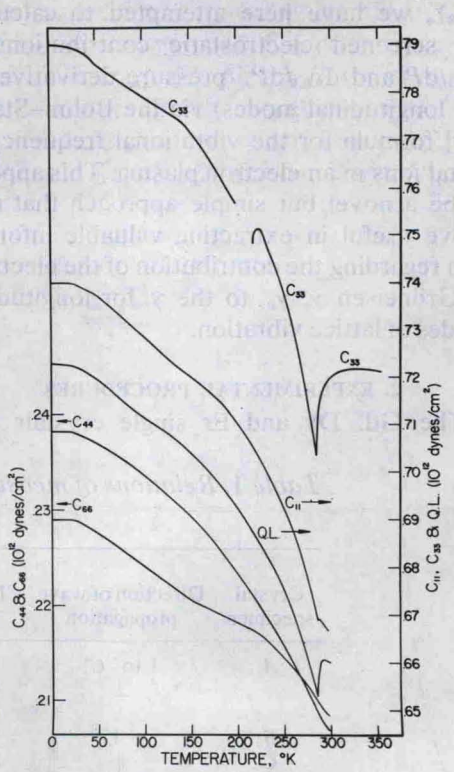

Fig. 1. Elastic moduli at zero magnetic field vs temperature for Gd, where $T_c = 291$°K. Anomaly in c_{33} at ~ 215°K is related to change in direction of easy magnetization.

the elastic moduli at zero field and pressure are shown in Fig. 2. Data published by Rosen and Klimker [9] show similar, but significantly different, effects. The differences between Fig. 2 and Rosen's data are primarily in the variation of c_{12}; consequently, the variations of the compressibilities $\beta_{\|}$ and $\beta_{\perp}$ with turn angle and structure, that are calculated from the Fig. 2 data, are considerably different than given by Rosen. In the present context, however, there appears no indication that magnetic ordering has any influence on the second order elastic moduli at 298°K.

The magnetic structures in Er are even more complex. The spontaneous ferromagnetic phase, with $T_c = 20$°K, contains a spiral component. The ferromagnetic component transforms to an antiferromagnetic arrangement, between 20 and 53°K, and a modulated moment arrangement between 53 and 80°K. The effects of the ordering on the elastic moduli are shown in Fig. 3. These effects are clearly not evident at 298°K.

The values of the second order elastic stiffness moduli at 298°K are listed in Table 2. We include here the data for Ho as given by Palmer and Lee [8]. Included in Table 2 are the values of the density [18] that are used for computing the moduli. The calculated adiabatic and isothermal bulk moduli, K_s and K_T, and also given and the last column gives the parameters $(\beta_{\|}-\beta_{\perp})/\beta_V$ calculated from isothermal values of the compressibilities. The latter parameter is that used for computing equation (3). The variations of the data with increasing atomic number (Gd → Er) are noteworthy. The c/a ratio decreases whereas the density increases because of the so-called lanthanide contraction associated with the addition of electrons to the $4f$ shell. There is

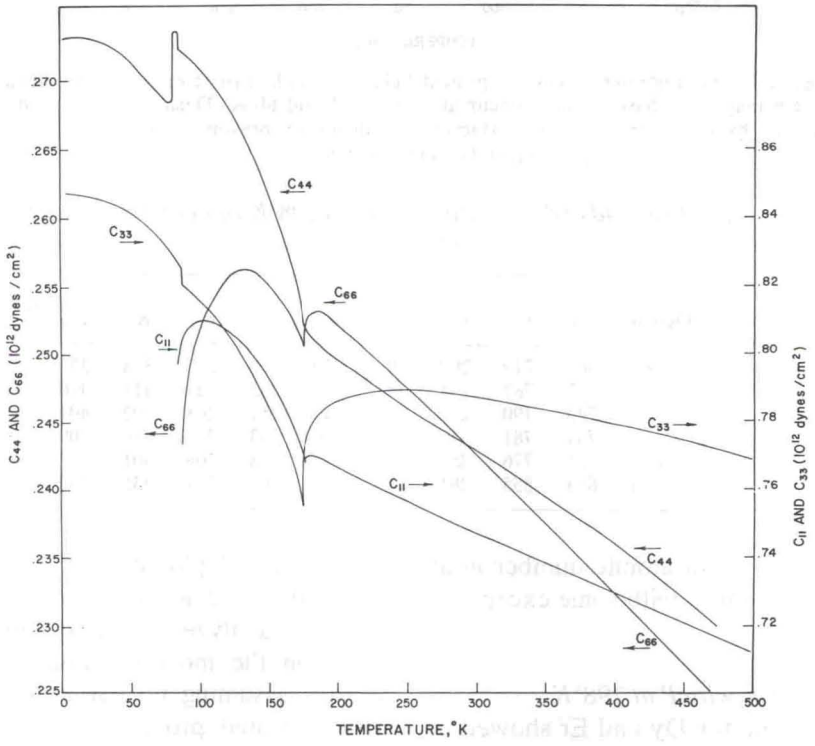

Fig. 2. Temperature dependence of the principal elastic moduli of Dy at zero magnetic field. $T_N = 179$°K and $T_c = 87$°K. Absence of data for c_{11} and c_{66} at $T < 85$°K is result of spontaneous macroscopic distortion by anisotropic magnetostriction.

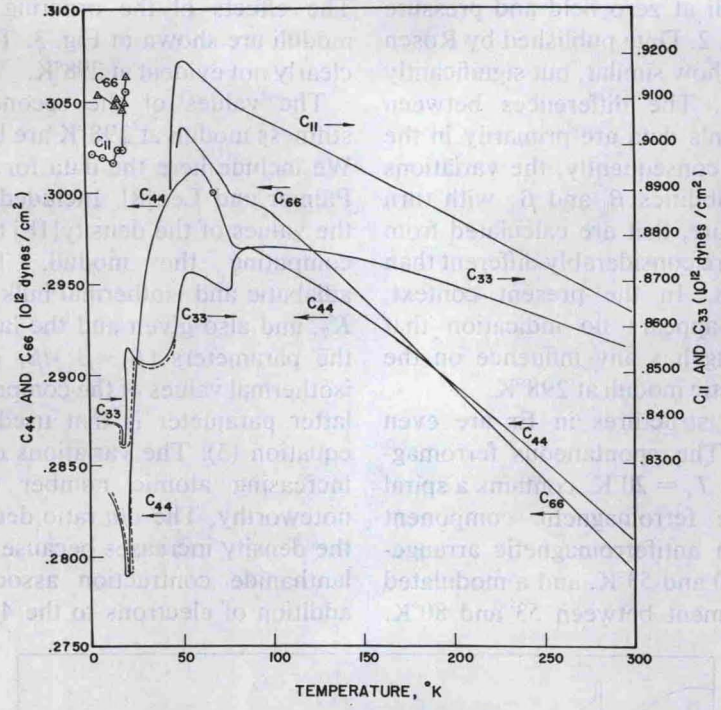

Fig. 3. Temperature dependence of principal elastic moduli in Er at zero magnetic field, where magnetic phase changes occur at ~20, ~53 and 80°K. Dashed lines indicate thermal hysteresis in $T_c \sim 20$°K. Macroscopic distortion prevented measurements of c_{11} and c_{66} in spiral phase.

Table 2. Values of second order elastic moduli at 298°K of heavy rare earth metals (Kbars)

	c/a	Density	c_{11}	c_{33}	c_{44}	c_{66}	C_H	c_{12}	c_{13}	K_s	K_T	$\left(\frac{\beta_\parallel - \beta_\perp}{\beta_V}\right)_T$
Gd	1·590	7·888	667	719	207	208	250	250	213	378	373	+0·007
Dy(F)	1·573	8·560	747	787	243	243	278	262	223	411	410	−0·005
Dy(R)		8·545	743	790	255	246	290	251	208	402	401	−0·009
Dy(P)		8·560	731	781	240	239	276	253	223	410	409	−0·015
Ho	1·570	8·800	761	776	257	256	290	248	206	401		+0·019
Er	1·569	9·064	863	855	281	279	328	305	227	455	450	+0·043

a general increase with atomic number in all of the c_{ij} and K values, with some exceptions for the Ho data.

(b) *Variations of c_{ij} with P at 298°K*

Plots of the data for Dy and Er showed no significant or systematic departure from linear relations between the c_{ij} and pressure. The Gd data showed small but significant curvature for the c_{33} vs P plot at $P > 2$ Kbar and for c_{44} at $P = 0$ and 2 Kbar. All of the data were, however, analyzed by least square statistics to obtain the most probable values for the dc_{ij}/dP, assuming no curvature. The results with indicated probable errors are given in Table 3. The similarities and differences in the effects of pressure on the c_{ij} of the three metals are evident in the pressure derivatives

Table 3. *Measured values of* $dc_{ij}/dP = c'_{ij}$ *at* 298°K, *for Gd, Dy and Er*

	Gd	Dy	Er
c'_{11}	3·018 ± 0·02	3·092 ± 0·006	4·768 ± 0·020
c'_{33}	5·726 ± 0·05	5·331 ± 0·008	5·448 ± 0·018
c'_{44}	0·185 ± 0·012	0·434 ± 0·001	0·949 ± 0·005
c'_{66}	0·377 ± 0·002	0·408 ± 0·002	0·853 ± 0·012
c'_H	0·435 ± 0·028	0·457 ± 0·070	1·663 ± 0·033
c'_{12}	2·26 ± 0·02	2·277 ± 0·006	3·062 ± 0·044
c'_{13}	3·53 ± 0·05	3·32 ± 0·1	2·16 ± 0·04
K'_s	3·320 ± 0·039	3·214 ± 0·054	3·302 ± 0·02
K'_T		3·228 ± 0·044	3·256 ± 0·25

but become considerably sharper when the derivatives are normalized with respect to initial values of the c_{ij} and volume compressibility. The two types of parameters are related as follows:

$$\pi_{ij} = \frac{\mathrm{d} \ln c_{ij}}{\mathrm{d} \ln V} = \frac{V}{c_{ij}}\left(\frac{\mathrm{d}c_{ij}}{\mathrm{d}P}\right)\frac{\mathrm{d}P}{\mathrm{d}V} = -\frac{K_T}{c_{ij}}\left(\frac{\mathrm{d}c_{ij}}{\mathrm{d}P}\right). \quad (5)$$

The 298°K values of π_{ij} for c_{11}, c_{33}, c_{44}, c_{66}, c_H, K_s and K_T computed from the above equation with the zero pressure values of K_T and c_{ij}, are given in Table 4. The probable errors given in Table 4 are based on the probable errors in $\mathrm{d}c_{ij}/\mathrm{d}P$ and estimated probable errors of 1 per cent total in each of the (K_T/c_{ij}) factors. The values of π_{33}, π_{K_s}, and π_{K_T} show only small variations between all 3 metals, with the values of Gd being slightly larger in magnitude. The π_{11} values for Gd and Dy are identical as are the values of π_{66} and π_{C_H}. In sharp contrast, π_{11} and π_{66} for Er are considerably greater. The π_{44} values are distinguished by the large differences in this parameter among the 3 metals.

Since we will be concerned with the possibility that the π_{ij} values for Gd are influenced by the spatial coherent magnetic order fluctuations at 298°K, measurements of c_{ij} for Gd were also carried out in the ferromagnetic phase, at 273°K. The results for ferromagnetic Gd are given in Table 5. By comparison with Table 4, it is noted that the magnetic order at 273°K reduces π_{11}, π_{33} and π_{K_s} very significantly, but the effects on π_{44} and π_{66} are quite small. The π_{44} values at 273°K and at 298°K are the same within the quoted errors.

4. DISCUSSION

The values of $\mathrm{d}K_s/\mathrm{d}P$ for all three metals and $\mathrm{d}K_T/\mathrm{d}P$ for Dy and Er are clearly smaller than Anderson's [19] 'lower limit' of 3·5 and are indeed smaller than reliable published values of $\mathrm{d}K_s/\mathrm{d}P$ for any solid including that for Na, where the ultrasonic data [2] gives $\mathrm{d}K_s/\mathrm{d}P \sim 3{\cdot}3$. The significance of the small $\mathrm{d}K_s/\mathrm{d}P$ is that one can be reasonably assured that the short range ion core repulsive contribution to the other compressional moduli, the shear moduli and their volume derivatives are relatively minor. We can then be fairly confident that an analysis of the values for $\mathrm{d}c_{44}/\mathrm{d}P$, $\mathrm{d}c_{66}/\mathrm{d}P$, and $\mathrm{d}C_H/\mathrm{d}P$ in terms of electrostatic and band structure contributions alone is a reasonably good model for Gd, Dy and Er metals. In view of the almost identical values for $\mathrm{d}K_s/\mathrm{d}P$ for the three metals it seems reasonably safe to conclude that the small core model holds for the elastic moduli and cohesive energy of all the heavy rare earth metals.

(a) *Analyses of* π_{44}, π_{66}, *and* π_{C_H}

The values of the electrostatic contributions to the volume derivatives of the shear moduli

Table 4. *Measured values of* $\pi_{ij} = d \ln c_{ij}/d \ln V$ *at* 298°K, *for Gd, Dy and Er*

	π_{11}	π_{33}	π_{44}	π_{66}	π_{C_H}	π_{K_s}	$\pi_{K_T=K'_T}$
Gd	−1·713 ± 0·03	−3·013 ± 0·06	−0·339 ± 0·025	−0·690 ± 0·10	0·648 ± 0·05	−3·283 ± 0·39	
Dy	−1·701 + 0·02	−2·783 ± 0·03	−0·734 ± 0·010	−0·690 ± 0·01	0·674 ± 0·10	−3·214 ± 0·054	−3·228 ± 0·044
Er	−2·510 ± 0·03	−2·895 ± 0·04	−1·538 ± 0·02	−1·390 ± 0·03	2·28 ± 0·068	−3·266 ± 0·021	−3·256 ± 0·025

Table 5. Values of $dc_{ij}/dP = c'_{ij}$ and $\pi_{ij} = d\ln c_{ij}/d\ln V$ for ferromagnetic Gd at 273°K, no external magnetic field. $(K_T)_{P=0} =$ 372·1 kbar

Modulus →	c_{11}	c_{33}	c_{44}	c_{66}
c'_{ij}	2·436 ± 0·016	3·841 ± 0·017	0·209 ± 0·011	0·338 ± 0·003
π_{ij}	−1·338 ± 0·023	−1·989 ± 0·028	−0·369 ± 0·024	−0·596 ± 0·012

	c_{12}	c_{13}	K_s	C_H
c'_{ij}	1·75 ± 0·016	2·01 ± 0·06	2·67 ± 0·03	0·042
π_{ij}	−2·56 ± 0·05	−5·36 ± 0·16	−2·64 ± 0·03	

of Gd, Dy and Er are given in Table 6 as calculated from equation (3). The values of M_{ij} and $(\partial M_{ij}/\partial[c/a])_V$ are taken directly from Cousins' computations [5]. For $c/a < 1{\cdot}65$ the M_{44}, M_{66} and M_{C_H} are linearly related to c/a and $(\partial M_{44}/\partial[c/a])_V$ is a factor of four larger than the next highest derivative, $(\partial M_{C_H}/\partial[c/a])_V$. The calculated values for four other hcp metals, Mg, Be, Zr and Ti are listed for comparison and the absolute differences between the electrostatic and observed values of π_{44}, π_{66} and π_{C_H} are also given [4, 20, 13, 10]. We note that the observed π_{44} and π_{66} values for Er (Table 4) are within 5 per cent of being the same as the respective electrostatic contributions. In contrast, the $(\pi_{44} - \pi^e_{44})$ values for Gd and Dy are about 1/3 and 2/3, respectively, of π^e_{44}. The $(\pi_{66} - \pi^e_{66})$ values for Gd and Dy are identical and about 50 per cent of π^e_{66}. The contrast between Er and the other two rare earths is further emphasized in the π_{C_H} values where the $(\pi_{C_H} - \pi^e_{C_H})$ are positive and identical within the errors, given in Table 4, for Gd and Dy, but negative for Er.

If we assume that electrostatic and band structure contributions to the shear moduli give clearly independent contributions to the c_{ij} values we have the following equation:

$$\pi_{ij} = \frac{\pi^e_{ij} \cdot c^e_{ij} + \pi^b_{ij} c^b_{ij}}{c_{ij}} \qquad (6)$$

where c^b_{ij} and π^b_{ij} represent the band structure contributions. If equation (6) is used, the weighted contribution of π^e_{ij} to the observed π_{ij} depends on the value of c^e_{ij}, computed from equation (1). It is thus necessary to define the effect valence, Z, making the partition between weighted π^e_{ij} and weighted π^b_{ij} somewhat arbitrary. It is nevertheless of some value to

Table 6. Electrostatic contributions to π_{44}, π_{66} and π_{C_H} for several hcp metals, as calculated from equation (3)

	π^e_{44}	$\pi_{44} - \pi^e_{44}$	π^e_{66}	$\pi_{66} - \pi^e_{66}$	$\pi^e_{C_H}$	$\pi_{C_H} - \pi^e_{C_H}$
Gd	−1·388	1·049	−1·337	0·647	−1·340	0·692
Dy	−1·303	0·569	−1·333	0·642	−1·329	0·655
Er	−1·609	0·071	−1·360	0·03	−1·378	−0·902
Mg	−1·513	−1·807	−1·341	−1·445	−1·346	−2·500
Be	−1·103	−0·60	−1·312	−0·447	−1·298	−0·289
Zr	−0·945	1·60	−1·300	0·602	−1·282	0·837
Ti	−1·491	0·296	1·341	0·01	−1·348	−0·458

assign $Z = 3$ to all three rare earth metals and thus estimate the proximity of the Er results to the pure electrostatic case assuming $dZ/dV = 0$. The results of calculating the weighted π_{ij}^e contributions to π_{44}, π_{66}, and π_{C_H} are given in Tables 7, 8 and 9, respectively. We note that the values of c_{44}^e, as calculated from $Z = 3$ and the M_{44} values computed by Cousins, are in fair agreement with the observed values of c_{44} in Gd, Dy and Er. The ratio $R_{44}^e = c_{44}^e/c_{44}$ is a useful gauge of the relative electrostatic and observed values and is carried through to Tables 8 and 9 for the c_{66}^e and C_H^e contributions.

The near electrostatic character of the shear moduli of Er is reflected consistently in the weighted contributions to the π_{ij} values, where the difference

$$\pi - \pi^e R^e = \pi^b R^b \qquad (7)$$

becomes a useful parameter for estimating the band structure contributions to the observed

Table 7. Evaluation of weighted electrostatic and band structure components to π_{44}, from equation (6)

	Z	c_{44}^e	$R_{44}^e = c_{44}^e/c_{44}^0$	$\pi_{44}^e R_{44}^e$	$\pi_{44}^b R_{44}^b$	π_{44}^b	dc_{44}^b/dP
Gd	3	283	1·29	−1·79	+1·45	−5·00	−0·84
Dy	3	323	1·25	−1·63	+0·89	−3·56	−0·56
Er	3	339	1·14	−1·83	+0·29	−2·07	−0·19
Mg	2·168	210	1·14	−1·72	−1·60	+11·48	+0·66
Be	2·137	1021	0·62	−0·68	−1·02	−2·84	+1·5
Zr	4	796	2·19	−2·07	+2·73	−2·29	−1·05
Ti	4	1179	2·32	−3·46	+2·27	−1·72	−1·08

Table 8. Evaluation of weighted electrostatic and band structure components to π_{66}

	c_{66}^e	R_{66}^e	$\pi_{66}^e R_{66}^e$	$\pi_{66}^b R_{66}^b$	π_{66}^b	dc_{66}^b/dP
Gd	405	1·72	−2·30	+1·61	−2·24	−1·02
Dy	429	1·59	−2·12	+1·43	−2·42	−0·98
Er	445	1·47	−2·00	+0·61	−1·30	−0·49
Mg	352	1·87	−2·51	−0·28	+0·32	+0·15
Be	1333	0·98	−1·29	−0·47	−2·35	+0·54
Zr	1153	2·61	−3·39	+2·69	−1·67	−1·25
Ti	1664	3·73	−5·00	+3·65	−1·34	−1·52

Table 9. Evaluation of electrostatic and band structure components to π_{C_H}

	C_H^e	R_H^e	$\pi_H^e R_H^e$	$\pi_H^b R_H^b$	π_H^b	dC_H^b/dP
Gd	559	2·24	−3·00	+2·35	−1·89	−1·37
Dy	581	2·01	−2·67	+2·00	−1·98	−1·40
Er	600	1·74	−2·40	+0·12	−0·16	−0·09
Mg	502	2·22	−2·99	−0·88	+0·72	+0·58
Be	1799	1·116	−1·45	−0·14	+1·20	+0·20
Zr	1597	3·10	−3·97	+3·53	−1·68	−1·92
Ti	2290	3·71	−5·00	+3·19	−1·18	−1·84

π. For Er the $\pi^b R^b$ difference does not exceed 1/3 of $\pi^e_{ij} R^e_{ij}$ for any one of the three moduli, whereas a relatively large $\pi^R_{ij} R^b_{ij}$ is necessary to account for at least one of the values observed for each of the other metals listed. Important examples of the latter are the π_{44} values for Mg and Be, where $\pi^b_{44} R^b_{44} \geqslant \pi^e_{44} R^e_{44}$.

Other interpretations of the data may be equally plausible at the present state of the theory of the rare earth metals. It is, for example, possible that $dZ/dV \neq 0$, thus contributing to π^e_{ij} in a positive way, i.e. making π^e_{ij} more negative by an increase in effective electron charge density in the spaces between the ions. The results for Er are, however, remarkably consistent with a simple Coulomb model with $dZ/dV = 0$. Since the highest magnetic ordering temperatures in Gd and Dy are higher than in Er, i.e. closer to the temperature of the present measurements, one might suspect that interactions between the conduction band and the 4*f* electrons are reflected in the Gd and Dy results. A direct effect of short range magnetic ordering on the shear modulus results seems improbable, however, since we see in Table 5 that the observed π_{44} and π_{66} of Gd at $T < T_c$ are not greatly different than in the paramagnetic phase.

(b) *Analysis of π_{11} and π_{33}*

It can be seen in Table 4 that the π values for the longitudinal stiffnesses, c_{11} and c_{33}, are considerably larger than those for the shear moduli. This is the usual case for solids and is qualitatively understood as a result of the fact that volume changes are produced by compressional waves but not shear waves. There will thus be a large contribution from the free electrons in the metal even when the core repulsion is relatively small. In the present case, it appears proper to consider the coupled plasma model of Bohm and Staver in which the electron-lattice interaction is derived from the screening by the free electrons of the charge produced by ionic motion [12, 21]. In this model the ion-core interaction is pure Coulombic and the phonon frequencies become wave number dependent because of the electron response. The result is that the sound velocity for a longitudinal wave is given as

$$V_l^2 = \left[\frac{m}{3M} Z\right] V_f^2. \tag{8}$$

Here M and Z are the ionic mass and charge and m and V_f are the electron mass and velocity, respectively. Since $V_f^2 = 2E_f/m$, where E_f is the Fermi energy, the sound velocity that is given by the Bohm–Staver equation will depend on the assumed valence as well as the Fermi energy, E_f. The general history of this equation [21] shows that it does indeed give reasonably good agreement, i.e. within 10 per cent, in the case of the alkali metals, where $Z = 1$ and E_f is computed from the free electron gas model. In other metals, including Mg, the deviation from observed values of longitudinal velocities exceeds 20 per cent. It is, therefore, significant that the values of V_l calculated from equation (10) for Gd, Dy, and Er, with $Z = 3$ and E_f values calculated for the free electron gas, are remarkably close to the observed longitudinal sound velocities in either the [0001] directions or in perpendicular directions, as shown in Table 10. In all cases the free electron calculated V_l are within 3 per cent of the observed values. The second values of E_f noted in the

Table 10. *Comparison of Bohm–Staver longitudinal sound velocity with measured values for Gd, Dy and Er at* 300°K

Metal	E_f (Rydbergs)	V_l calculated (cm/sec) $\times 10^{-5}$	V_{11}	V_{33}
Gd	0·540*	3·002	2·91	3·02
	0·425 (Ref. [23])	2·66		
Dy	0·558*	3·002	2·95	3·03
	0·450 (Ref. [23])	2·696		
Er	0·568*	2·987	3·09	3·07
	0·452 (Ref. [23])	2·664		

*Free electron gas model.

table are from relativistic APW calculations of Keeton and Loucks [22] and the corresponding V_l values, again for $Z = 3$, are within 12 per cent of the observed.

The calculation of the volume derivatives of c_{11} and c_{33} from equation (10) is subject to considerable question because of the assumption of a spherical Fermi surface. In this overly simplified model the volume dependence of the velocity is derived entirely from the change in E_f on the basis of a spherical Fermi surface and values of π_{ij} for longitudinal modes turns out to be

$$\pi_l = -\frac{5}{3}.$$

It is, however, of interest to note that the observed π_{11} values for Gd and Dy given in Table 4 are very close to $-5/3$ and that the π_{11} value for Er and π_{33} values for all three metals are within a factor of two of the spherical Fermi surface model. There is, then, qualitative value in reformulating the free electron gas model so as to relate π_{ij} to the volume dependence of the density of electron states, $N(E_f)$. We then find that

$$\pi_l = -1 - \frac{\mathrm{d} \ln N(E_f)}{\mathrm{d} \ln V} \qquad (9)$$

where in the free electron model

$$\frac{\mathrm{d} \ln N(E_f)}{\mathrm{d} \ln V} = \frac{2}{3}.$$

The latter quantity is of particular interest [23] in understanding the observed effects of hydrostatic pressures on T_c and or T_N and it is therefore of interest to propose some reasonable estimates of this number from our data. The anisotropy, i.e. differences between π_{11} and π_{33}, presents a problem in literal interpretation of the data. If the anisotropy is indeed caused by the $\mathrm{d} \ln N(E_f)/\mathrm{d} \ln V$ term, we conclude that the change in $N(E_f)$ with volume change is considerably larger along the c axes of Gd and Dy then in perpendicular directions. This situation is, evidently not related to $\mathrm{d}(c/a)/\mathrm{d}V$, is perhaps related to the symmetry of the conduction band energies (and their proximity) to E_f. For Gd and Dy we conclude that $0{\cdot}7 < \mathrm{d} \ln N(E_f)/\mathrm{d} \ln V < 2{\cdot}0$, whereas for Er, $1{\cdot}5 < \mathrm{d} \ln N(E_f)/\mathrm{d} \ln V < 2{\cdot}0$.

(c) *Analysis of the Grüneisen parameters*

One of the unique characteristics of the hcp rare earth metals are the relatively small values of the Grüneisen parameter, γ, that is obtained from thermal expansion measurements, as follows:

$$\gamma(\alpha_V) = \frac{\alpha_V K_T}{\rho C_V} = \frac{\alpha_V K_s}{\rho C_p} \qquad (10)$$

where α_V is the volume thermal expansion coefficient and C_v and C_p are the constant volume and constant pressure specific heat coefficients, respectively. Since all of the factors that enter into the above equation are sensitive to magnetic ordering, the characterization of the lattice contribution to $\gamma(\alpha_V)$ of the paramagnetic phases of the rare earths is not straightforward. The values of $\gamma(\alpha_V)$ given in Table 11 illustrate the problem encountered for Gd. Gschneidner's values [24, 25] evidently represent γ at 298°K, based on α_V and C_p values that are definitely influenced by the fluctuations in magnetic order that are present at 10°K above T_c. The third value listed for $\gamma_H(\alpha_V)$ is obtained from α_V, K_T, ρ, and C_v at 673°K [27, 28], where all of the parameters are more likely to represent the paramagnetic lattice properties. The values of $\gamma_H(\alpha_V)$ for Dy and Er as calculated from the K_s values given in Table 2 and the α_V and C_p values [26–28] at 298°K are also listed in Table 11, along with those given by Gschneidner's [24, 25].

Direct estimates of γ can be arrived at by various means from the relation.

$$\bar{\gamma} = -\frac{\mathrm{d} \ln \bar{\omega}}{\mathrm{d} \ln V} \qquad (11)$$

Table 11. *Comparison of the average Grüneisen parameter* $\gamma_H(\alpha_V)$, *as determined from thermal expansion and specific heat data, with that calculated from the measured* dc_{ij}/dP, $\bar{\gamma}_H$, *and the adjusted* dc_{ij}/dP [*equation* (17*b*)], $\bar{\gamma}_H^*$. *The thermal expansion coefficients and* c_p *values used for evaluating* $\bar{\gamma}_H(\alpha_V)$ *are listed*

	$\gamma_H(\alpha_V)$	$\bar{\gamma}_H$	$\bar{\gamma}_H^*$	$\alpha_\parallel \times 10^{-6}$/°K	$\alpha_\perp \times 10^{-6}$/°K	$\alpha_V \times 10^{-4}$/°K	C_p cal/g, °K
Gd	0·52 (Ref. [24])						
	0·55 (Ref. [25])						
	0·79	0·370	0·82	13·0	6·3	25·6	0·0374
Dy	0·78 (Ref. [24])						
	0·68 (Ref. [25])						
	0·83	0·42	0·83	15·6	7·13	29·9	0·0412
Er	1·01 (Ref. [24])						
	0·88 (Ref. [25])						
	1·08	0·80	1·20	20·92	7·89	36·7	0·0405

where $\bar{\omega}$ represents the average vibrational frequency of the lattice modes. The method proposed by Sheard for calculating $\bar{\gamma}$ [see equation (4)] from the pressure derivatives of the c_{ij} has been shown to give reasonably good agreement with $\gamma(\alpha_V)$ obtained from highly precise measurement of α_V at low and high temperatures in various solids, including Mg and Cd in the family of *hcp* metals [11, 29]. This method is in principle an approximation based on the assumption that only low frequency acoustic modes contribute to $\bar{\gamma}$, but its success in giving good agreement with $\gamma(\alpha_V)$ at high temperatures indicates either that $\gamma(\alpha_V)$ at high temperatures is in fact dominated by the acoustic modes or that $\bar{\gamma}$ evaluated from low frequency acoustic modes is also representative of $\bar{\gamma}$ for the high frequency modes.

The procedure for equating the dc_{ij}/dP values to $\bar{\gamma}$ in uniaxial crystals has been given by Gerlich [29], as an approximation from the general strain approach given by Brugger [30]. The individual mode γ's for hydrostatic strain are obtained from a variation of equation (4), where the factor $-1/6$ is replaced by $-1/2$ plus the ratio of the linear compressibility to volume compressibility in the direction of wave propagation, q. The mode γ's, $\gamma^P(q)$ for each of the three wave modes for a given propagation, are obtained from solutions of the Christoffel eigen matrix, where the matrix elements are functions of the principal dc_{ij}/dP given as $dC_p(q)/dP$, where p represents the displacement polarization for a given wave mode. The general equation for computing $\gamma^P(q)$ is then

$$\gamma^P(q) = \frac{\beta_q}{\beta_v} - \frac{1}{2}\left[1 + \frac{d \ln C_p(q)}{d \ln V}\right] \quad (12)$$

where

$$\frac{d \ln C_p(q)}{d \ln V} = \pi^P(q) = -\frac{K_T}{C_p(q)} \frac{dC_p(q)}{dP}, \quad (13)$$

and for computing the average value of $\gamma^P(q)$ at temperatures where all the lattice vibrational modes contribute to C_v, the specific heat,

$$\bar{\gamma}_H = \sum_1^{3N} \gamma^P(q)/3N \quad (14)$$

where N represents the number of q directions for which the $\gamma^P(q)$ have been calculated. For sufficient N and systematic choices of q, the computed $\bar{\gamma}_H$ should provide a reasonably good approximation to the $\gamma(\alpha_V)$ determined from α_V at high temperatures, if the principal dc_{ij}/dP are derived strictly from the volume dependence of the c_{ij}.

If, however, the measured dc_{ij}/dP contain a significant contribution from the change in

the c/a ratio with pressure, the computed $\bar{\gamma}_H$ cannot be expected to agree with $\gamma(\alpha_V)$ unless the atomic configurational change with volume, $\mathrm{d}(c/a)/\mathrm{d}V$, is the same during thermal expansion as in the application of hydrostatic pressure.

Since

$$\left(\frac{\partial \ln (c/a)}{\partial \ln V}\right)_T = \frac{\beta_\parallel - \beta_\perp}{\beta_v} \tag{15}$$

during hydrostatic compression and

$$\left(\frac{\partial \ln (c/a)}{\partial \ln V}\right)_P = \frac{\alpha_\parallel - \alpha_\perp}{\alpha_V} \tag{16}$$

during thermal expansion, one is in a position to predict whether $\gamma_H = \gamma_H(\alpha_V)$, if $\mathrm{d}c_{ij}/\mathrm{d}(c/a)$ can be evaluated. Thus one finds for Mg, where $(\partial(c/a)/\alpha_V)_T \simeq (\partial(c/a)/\alpha_V)_P$, the evaluation of γ_H from the experimental $\mathrm{d}c_{ij}/\mathrm{d}P$ gives excellent agreement with $\bar{\gamma}_H(\alpha_V)$. In Zr and Ti[10], however, the experimental $\mathrm{d}c_{ij}/\mathrm{d}P$ lead to large differences between γ_H and $\gamma_H(\alpha_V)$, primarily because of the small values of $\mathrm{d}c_{44}/\mathrm{d}P$. The present authors have shown that the assumption of a negative $\mathrm{d}c_{44}/\mathrm{d}(c/a)$ contribution accounts for the small values of $\mathrm{d}c_{44}/\mathrm{d}P$ and can also account for a major part of the difference in $\bar{\gamma}_H$ and $\gamma_H(\alpha_V)$ when the differences between $(\partial c/a/\partial V)_T$ and $(\partial(c/a)/\partial V)_P$ are considered[10]. The procedure that was used for the latter consideration requires only the following simple adjustment of the $\mathrm{d}c_{ij}/\mathrm{d}P$ values that are used for computing $\bar{\gamma}_H$:

$$\left(\frac{\mathrm{d}c_{ij}}{\mathrm{d}P}\right)^* = (\mathrm{d}c_{ij}/\mathrm{d}P)_{\text{obs.}} - \left(\frac{\partial c_{ij}}{\partial c/a}\right)_V \left(\frac{\partial c/a}{\partial P}\right)_T + \frac{\partial c_{ij}}{\partial c/a}\left(\frac{\partial c/a}{\partial V}\right)_p \frac{\mathrm{d}V}{\mathrm{d}P} \tag{17a}$$

$$= \left(\frac{\mathrm{d}c_{ij}}{\mathrm{d}P}\right)_{\text{obs.}} + \beta_V \frac{c}{a}\left(\frac{\partial c_{ij}}{\partial c/a}\right)_V \times \left[\left(\frac{\beta_\parallel - \beta_\perp}{\beta_V}\right) - \left(\frac{\alpha_\parallel - \alpha_\perp}{\alpha_V}\right)\right] \tag{17b}$$

where $(\mathrm{d}c_{ij}/\mathrm{d}P)^*$ is the effective value to be used in computing the $\gamma^P(q)$. In view of the very large values of $(\alpha_\parallel - \alpha_\perp)$ that are found in the *hcp* rare earth metals, the comparisons of $\bar{\gamma}_H$ and $\bar{\gamma}_H(\alpha_V)$ for Gd, Dy and Er provide a severe test of the reasoning that leads to equation (17b). We see immediately that the computed values of $\bar{\gamma}_H$ from the observed values of the $\mathrm{d}c_{ij}/\mathrm{d}P$, using equations (12), (13) and (14), are considerably smaller than $\gamma_H(\alpha_V)$. Since the $(\beta_\parallel - \beta_\perp)/\beta_V$ values are relatively small, the $\bar{\gamma}_H$ evidently reflect the small volume dependence of the transverse $C_p(q)$ that are numerically dependent on π_{44} and π_{66} for all three metals. The wide differences between $\bar{\gamma}_H$ and $\bar{\gamma}_H(\alpha_V)$ may presumed to arise from the relatively large value of $\partial c^e_{44}/\partial(c/a)$, as given by Cousins[5]. For all three metals $\partial c^e_{44}/\partial(c/a) \sim 10\partial c^e_{66}/\partial(c/a)$, therefore a simple adjustment of the $\mathrm{d}c_{44}/\mathrm{d}P$ value for each metal, using equation (17b) and $[\partial c_{44}/\partial(c/a)] = Z^2/a_0 28 \times 10^{12}$ dynes/cm^2, should provide a semiquantitative test of our assumptions. These results are given in Table 11 as γ^*_H. The latter values give a reasonably good approximation to the $\gamma_H(\alpha_V)$ and lead to the conclusion that the $\gamma_H(\alpha_V)$ contain a significantly large contribution from the dependence of transverse mode frequencies on the c/a ratio.

(d) *Comparison of dK_T/dP with Bridgman's compression data*

The value of $(\partial K_T/\partial P)_T$ plays a central role in the equation of state. Anderson[31] has shown that the initial value of $\mathrm{d}K_T/\mathrm{d}P$ as determined from ultrasonic data as $P \to 0$, giving $(K'_T)_0$, can successfully predict the change of volume of many solids over a wide range of pressures, when used in conjunction with either the Murnaghan[32] or Birch[33] equations. The latter equations are derived from the expansion of the basic equation, $P = -\mathrm{d}\phi/\mathrm{d}V$, where ϕ is the strain energy. Using finite strain theory, Murnaghan's equation predicts the following relation

between V/V_0 and P:

$$\frac{V}{V_0} = [1 + (K_T')_0 P/(K_T)_0]^{-1/(K_T')_0}. \quad (18)$$

We should then find that equation (18) agrees with the direct measurements of volume changes in Gd, Dy and Er that were carried out by Bridgman [34] in 1954. Since the Bridgman measurements extend only to approximately 40 kbar the comparison is not a severe test of the Murnaghan equation and the agreement should be better than a comparison with very high pressure data, such as encountered with shock-wave results. This is indeed found to be true, as shown in Fig. 4, for Dy and Er. There are obvious differences for Gd at the higher pressure range that suggest that our use of $(K_s')_0$, rather than $(K_T')_0$ is not a good approximation. As stated in an earlier section, above, the calculation of K_T' from K_s' in this case is extremely difficult because of the proximity of the Curie temperature to room temperature i.e., the values of $\mathrm{d}\alpha_V/\mathrm{d}P$ or $\mathrm{d}\beta_V/\mathrm{d}T$ are subject to very large errors. We may conclude from Bridgman's data that $(K_T')_0$ is enhanced by the effects of the magnetic transition on K_T as well as on α_V.

The magnitude of the enhancement in Gd is quite large, as shown in Table 12, where the values of $\mathrm{d}K_T'/P$ derived from Bridgman's data are compared with the ultrasonic values. Bridgman K_T' is that obtained from expressing the compression data as a polynomial in P, as follows:

$$V/V_0 = 1 - aP + bP^2$$

$$1/K_0 = a - 2bP$$

$$\mathrm{d}K_0/\mathrm{d}P = 2bK_0^2 = K_0'.$$

The reasonable agreement between the K_0' and K_T' values for Dy and Er indicates that a major part of the difference between K_0' and K_s' for Gd can be attributed to the isothermal–adiabatic conversion. We believe that this is the first experimental evidence that the $K_s' \rightarrow K_T'$ conversion, and thus the equation of state, can be subject to considerable error near magnetic

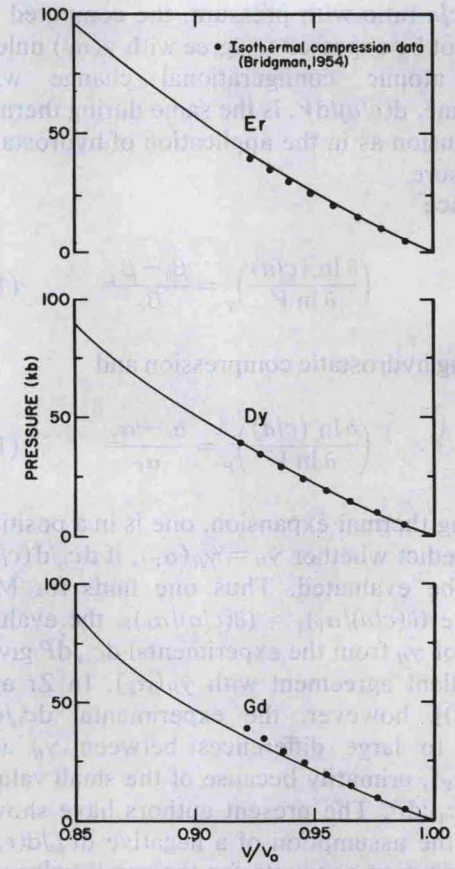

Fig. 4. Pressure-volume curves for Gd, Dy and Er obtained from the Murnaghan equation of state and $(K_T')_0$ values given in Table 12. (K_s' was used for Gd curve). Data points are from direct compression measurements by Bridgman.

Table 12. Comparison of ultrasonic K_T' with K_0' determined from Bridgman's compression data

Metal	K_0' (Ref. 34)	K_s' (Present work)	K_T'
Gd	4·517	3·283	
Dy	3·305	3·214	3·228
Er	3·634	3·302	3·256

transitions when the anomalous $d\alpha_V/dT$, dC_p/dT, and dK_s/dT factors are not carefully evaluated.

(e) *Pressure induced phase changes*

An alternative explanation for the deviation of Bridgman's data for Gd from the Murnaghan equation with K_s' is that a structural phase transition is induced near 25 kbar, as suggested by one of Bridgman's studies [35] and which seems to be indicated in more recent studies of Gd [36]. The deviations of Bridgman's data, shown in Fig. 4, are, however, gradually increasing from 10 kbar and show no clear indication of a sharp change in the equation of state as would be expected for a structural change. A more clear association between the equation of state and a phase transition is found in the case of Er, where Drickamer *et al.* [37], have measured the changes in lattice constants with pressure to 200 kbar. Distinct changes in the pressure derivatives of the c_0 and a_0 lattice constants occur at approximately 90 kbar. The diffraction data indicate that the high pressure phase has the double hcp symmetry. The P–V plot of the diffraction data for Er is shown in Fig. 5, where the Murnaghan equation and Bridgman's data are also shown for comparison. From $P = 0$ to $P = 94$ kbar, the Murnaghan equation with $(K_T')_0 = 3{\cdot}256$ falls well within the error bars of the diffraction data. At $P >$ 94 kbar the diffraction data show that the appropriate $(K_T')_0$ is considerably greater than that used in the Murnaghan equation.

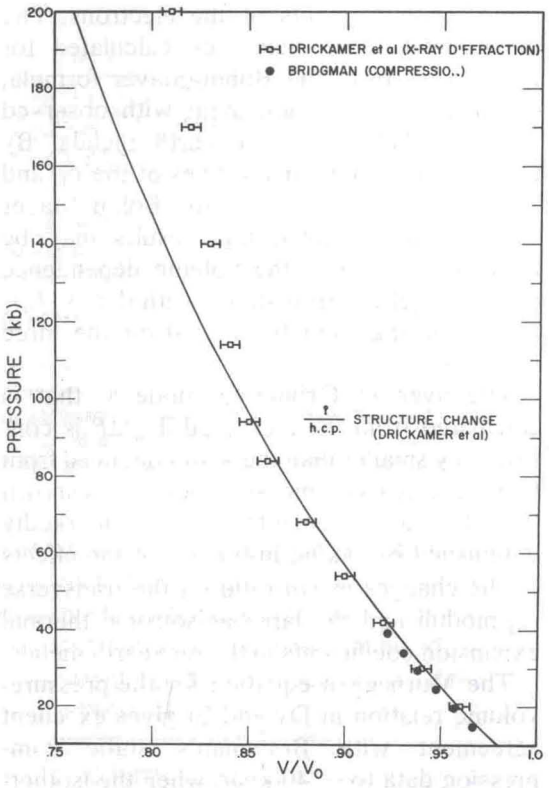

Fig. 5. Comparison of Murnaghan equation for Er with P–V data obtained from X-ray diffraction measurements up to 200 kbar. Question mark denotes that crystal structure at $P > 90$ kbar is not established.

5. SUMMARY

The pressure derivatives of the elastic moduli in the paramagnetic hcp rare earth metals, Gd, Dy and Er, have been used as a measure of the relative importance of the electrostatic forces in determining the elastic properties of lanthanide metals. For Er, the pressure derivatives of the shear moduli can be closely approximated by an electrostatic model, assuming no change in valence with volume but a change in the Coulomb sum parameter with c/a ratio. The results for Gd and Dy are quite similar to each other but different from Er. By deduction it is concluded that the band structure produces negative contributions to the pressure derivatives of the shear moduli in all three metals and that this contribution is considerably larger in Gd and Dy.

The pressure derivatives of the bulk moduli for the three metals are smaller than in other solids and indicate that the repulsive forces between ions can be safely neglected in understanding the elastic moduli.

The longitudinal wave velocities and their pressure derivatives are also interpreted on a nearly electrostatic model, where the ions are immersed in an electron sea and their vibrational frequencies are affected by the charge

screening movements of the electrons. The longitudinal wave velocities calculated for this model, from the Bohm–Staver formula, are in remarkable agreement with observed values in all three rare earth metals. By treating the volume derivatives of the c_{11} and c_{33} values on the basis of the Bohm–Staver equation it is shown that results may be understood through the volume dependence of density of electron states, with $\mathrm{d}\ln N(E_f)/\mathrm{d}\ln V$ varying from 0·7 to 2·0 for the three metals.

The average Grüneisen mode γ_i that is calculated from the measured $\mathrm{d}c_{ij}/\mathrm{d}P$ is considerably smaller than the $\gamma(\alpha_V)$ deduced from thermal expansion measurements. It is shown that the disagreements can be markedly diminished by taking into account the effects of the changes in c/a ratio on the transverse c_{44} moduli and the large anisotropic thermal expansion coefficients in the rare earth metals.

The Murnaghan equation for the pressure-volume relation in Dy and Er gives excellent agreement with Bridgman's static compression data to ~ 40 kbar, when the isothermal values of $\mathrm{d}K_T/\mathrm{d}P$ computed from the present data are used in the equation of state. For Gd there is significant disagreement above ~20 kbar. This may arise from a very large difference between $\mathrm{d}K_s/\mathrm{d}P$ and $\mathrm{d}K_T/\mathrm{d}P$ at 298°K. Because the Curie temperature occurs at 291°K, there are very large values of $\mathrm{d}\alpha_V/\mathrm{d}T$ and $\mathrm{d}C_p/\mathrm{d}T$ that are difficult to evaluate accurately and thus lead to large errors in calculating $\mathrm{d}K_T/\mathrm{d}P$. An alternative explanation is that a pressure induced phase change occurs in Gd at $P \sim 20$ kbar. It is shown that a phase change in Er near 90 kbar produces a relatively sharp deviation at $P > 95$ kbar between X-ray diffraction data of Drickamer *et al.*, and the Murnaghan equation.

Acknowledgements—Measurements of elastic moduli at temperatures below 273°K were carried out at Argonne National Laboratory, under auspices of the Division of Research, U.S. Atomic Energy Commission. Work supported by National Science Foundation grant GK-29750.

REFERENCES

1. See for example, ANDERSON O. J., *J. geophys. Res.* **75**, 2719 (1970).
2. DANIELS W. B. and SMITH C. S., in *The Physics and Chemistry of High Pressures*, p. 50, Gordon and Breach, New York (1963).
3. KI Y. H., THOMAS Jr. J. F. and GRANATO A. V., *Phys. Rev.* **153**, 764 (1967).
4. SCHMUNK R. E. and SMITH C. S., *J. Phys. Chem. Solids* **9**, 100 (1959).
5. COUSINS C. S. G., *J. Phys. C (Proc. Phys. Soc.)* **1**, 478 (1968).
6. FISHER E. S. and DEVER D. J., in *Proc. 6th Rare Earth Conf.*, Gatlinburg (1967), p. 522.
7. FISHER E. S. and DEVER D. J., *Trans. AIME* **239**, 48 (1967).
8. PALMER S. B. and LEE E. W., *Proc. R. Soc. Lond.* **A327**, 519 (1972).
9. ROSEN M. and KLIMKER H., *Phys. Rev.* **1B**, 3748 (1970).
10. FISHER E. S. and MANGHNANI M. H., *J. Phys. Chem. Solids* **32**, 657 (1971).
11. SHEARD F. W., *Phil. Mag.* **3**, 1381 (1958).
12. BOHM D. and STAVER T., *Phys. Rev.* **84**, 836 (1950).
13. FISHER E. S., MANGHNANI M. H. and SOKOLOWSKI T. J., *J. appl. Phys.* **41**, 2991 (1970).
14. An excellent review of magnetic structures in rare earth metals is given by W. C. Koehler, *J. appl. Phys.* **36**, 1078 (1965).
15. FISHER E. S., GOODMAN G. M., MANGHNANI M. H. and BENZING W. M., in *Les Propriétés Physiques des Solides sous Pression*, p. 311, Centre National de la Recherche Scientifique, Paris (1970).
16. DARNELL F. J. and CLOUD W. H., *J. appl. Phys.* **35**, 935 (1964).
17. BARTHOLIN H. and BLOCH D., *J. Phys. Chem. Solids* **29**, 1063 (1968).
18. SPEDDING F. H., DAANE A. H. and HERRMANN K. W., *Acta crystallogr.* **9**, 560 (1956).
19. ANDERSON O. L. and LIEBERMANN R. C., *Phys. Earth Planet. Interiors* **3**, 61 (1970).
20. SILVERSMITH D. J. and AVERBACH B. L., *Phys. Rev.* **1B**, 567 (1970).
21. PINES D., *Solid State Physics* (Edited by F. Seitz and D. Turnbull), Vol. 1, Academic Press, New York (1955).
22. KEETON S. C. and LOUCKS T. L., *Phys. Rev.* **168**, 672 (1968).
23. LIU S. H., *Phys. Rev.* **127**, 1889 (1962).
24. GSCHNEIDNER K. A., *Solid State Physics* (Edited by E. Seitz and D. Turnbull), Vol. 16, Academic Press, New York (1964).
25. GSCHNEIDNER K. A., *Rare Earth Alloys*, Van Nostrand, Princeton (1961).
26. SPEDDING F. H., HANAK J. J. and DAANE A. H., *J. less-common metals* **3**, 110 (1961).
27. DENNISON D. H., GSCHNEIDNER K. A. and DAANE A. H., *J. chem. Phys.* **44**, 4273 (1966).
28. SKOCHDOPOL R. E., GRIFFEL M. and SPEDDING F. H., *J. chem. Phys.* **23**, 2258 (1955).

29. GERLICH D., *J. Phys. Chem. Solids* **30**, 1638 (1969).
30. BRUGGER K., *Phys. Rev.* **137**, A1826 (1965).
31. ANDERSON O. L., *J. Phys. Chem. Solids* **27**, 547 (1966).
32. MURNAGHAN F. D., *Proc. Natn. Acad. Sci.* **30**, 244 (1944).
33. BIRCH F., *J. geophys. Res.* **57**, 227 (1952).
34. BRIDGMAN P. W., *Proc. Am. Acad. Arts Sci.* **83**, 3 (1954).
35. BRIDGMAN P. W., *Proc. Am. Acad. Arts Sci.* **32**, 83 (1953).
36. ROBINSON L. B., MILSTEIN F. and TAN S-I., *Physics of Solids at High Pressures*, p. 272. Academic Press, New York (1965).
37. DRICKAMER H. G., LYNCH CLENDENEN R. L. and PEREZ-ALBUERNE A., *Solid State Physics* (Edited by F. Seitz and D. Turnbull), Vol. 19, Academic Press, New York (1966).